

Enhancement of Si–O hybridization in low-temperature grown ultraviolet photo-oxidized SiO₂ film observed by x-ray absorption and photoemission spectroscopy

H. M. Tsai, S. C. Ray, C. W. Pao, J. W. Chiou,^{a)} C. L. Huang, C. H. Du, and W. F. Pong^{b)}
Department of Physics, Tamkang University, Tamsui 251, Taiwan

M.-H. Tsai
Department of Physics, National Sun Yat-Sen University, Kaohsiung 804, Taiwan

A. Fukano and H. Oyanagi
Photonics Research Institute, AIST, Tsukuba, Ibaraki 305-8568, Japan

(Received 23 August 2007; accepted 30 October 2007; published online 11 January 2008)

The dielectric properties associated with the electronic and bonding structures of SiO₂ films were examined using the Si *L*_{3,2}- and O *K*-edge x-ray absorption near-edge structures (XANES) and valence-band photoemission spectroscopy (VB-PES) techniques. The Si *L*_{3,2}- and O *K*-edge XANES measurements for the low-temperature grown UV-photon oxidized SiO₂ (UV-SiO₂) and the conventional high-temperature thermal-oxidized SiO₂ (TH-SiO₂) suggest enhancement of O 2*p*–Si 3*p* hybridization in UV-SiO₂. VB-PES measurements reveal enhancement of nonbonding O 2*p* and O 2*p*–Si 3*p* hybridized states. The enhanced O 2*p* and Si 3*p* hybridization implies a shortening of the average Si–O bond length, which explains an increase of the density and the improvement of the dielectric property of UV-SiO₂. © 2008 American Institute of Physics.

[DOI: [10.1063/1.2828144](https://doi.org/10.1063/1.2828144)]

I. INTRODUCTION

The electrical, electronic, and optical properties of SiO₂ have been extensively investigated in both crystalline and amorphous phases.^{1,2} Ultrathin SiO₂ films are important to Si-based semiconductor devices. However, a conventional high-temperature thermal-oxidized SiO₂ (TH-SiO₂) thin film is formed with a SiO_x layer at the Si–SiO₂ interface, which degrades insulating performance, reduces the voltage of electrical breakdown, and increases the leakage current in the SiO₂ thin film. Fukano and Oyanagi reported successful growth of high-*k* (high dielectric constant) ultrathin SiO₂ (<5 nm) films by means of vacuum ultraviolet (UV) photo-oxidation at low temperature to improve the dielectric limit of SiO₂,³ which clearly demonstrated that the dielectric property of UV photo-oxidized ultrathin SiO₂ (UV-SiO₂) film was better than that of the conventional TH-SiO₂ film. The UV-SiO₂ film is denser and has a higher dielectric constant than the conventional TH-SiO₂ film.³ The modified Auger parameter measured by Hirose *et al.*⁴ indicated that the dielectric constant of ultrathin (0.68–2.13 nm) SiO₂ films is identical to that of bulk SiO₂, suggesting that the strained structure of an ultrathin film does not substantially affect the SiO₂ dielectric constant. However, density-functional-theory calculations show that the dielectric constant of such a SiO₂ thin film is appreciably higher than that of bulk SiO₂.⁵ Modification of the Si–O network structure by rearrangement of

Si–O bonds and a change in the Si–O–Si bond angle was argued to strongly improve the dielectric properties of UV-SiO₂ films. The dielectric constant contains both the electronic and lattice contributions⁶ and therefore strongly correlates with the electronic and atomic structures of the dielectric materials.^{7–9} Thus, a microscopic understanding of the local electronic and bonding properties of O and Si atoms in ultrathin/thin SiO₂ films provides critical insight into the dielectric properties. For this purpose, measurements of UV-SiO₂ and TH-SiO₂ films using Si *L*_{3,2}- and O *K*-edge x-ray absorption near-edge structures (XANESs), valence-band photoemission spectroscopy (VB-PES), and x-ray diffraction (XRD) have been performed to elucidate the effects of low-temperature growth and UV photo-oxidation.

II. EXPERIMENTAL DETAILS

Si *L*_{3,2}-, O *K*-edge XANES, VB-PES spectra, and XRD were obtained at the National Synchrotron Radiation Research Center, Hsinchu, Taiwan. XANES data were obtained in the sample drain current and fluorescence modes, VB-PES spectra were obtained at an excitation of 130 eV and a base pressure of $\sim 5 \times 10^{-10}$ Torr, after the sample surface was cleaned by bombardment with Ar⁺. Two SiO₂ films with thicknesses of ~ 5 and 50 nm were synthesized on *p*-type Si(100) substrates by low-temperature (380 °C) UV photo-oxidation ($\lambda = 126$ nm) and high-temperature (1100 °C) thermal oxidation (wet), respectively. The average densities of UV- and TH-SiO₂ thin films were 2.32 and 2.20 g/cm³, respectively, obtained by x-ray reflectivity measurements with several photon wavelengths. The details of the preparation of these two films, their densities, electrical properties, and stoichiometries have been described elsewhere.³

^{a)}Permanent address: Department of Applied Physics, National University of Kaohsiung, Kaohsiung, Taiwan.

^{b)}Author to whom correspondence should be addressed. Electronic mail: wfpong@mail.tku.edu.tw. On leave at Advanced Light Source, Lawrence Berkeley National Laboratory, Berkeley, CA.

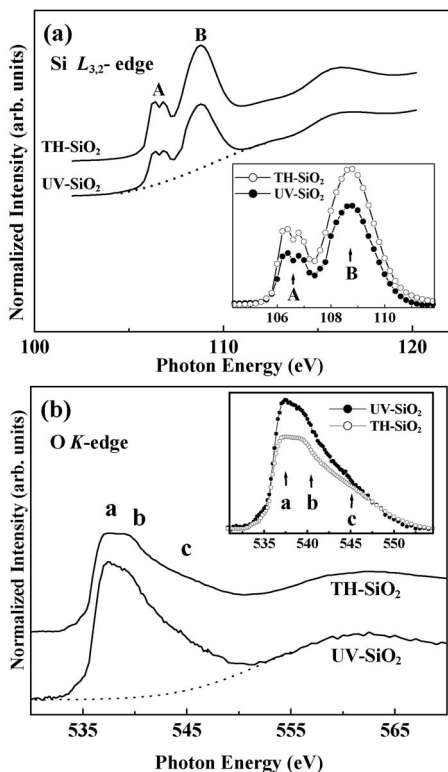


FIG. 1. Si $L_{3,2}$ - and (b) O K -edge XANES spectra of UV- and TH-SiO₂ films. The dotted line represents a best-fitted Gaussian background. The insets present magnified features A, B, and a, b, and c, after background subtraction.

III. RESULTS AND DISCUSSION

Figure 1(a) displays the normalized Si $L_{3,2}$ -edge XANES spectra of UV- and TH-SiO₂ films. The spectral features A and B of both UV- and TH-SiO₂ are separated by about 2.0 eV, which correspond to features A and C in Fig. 1(b) of Ref. 10 and features A and B in Fig. 1 of Ref. 11 in the Si $L_{3,2}$ -edge XANES spectrum of α -SiO₂. These features were also observed by Harp *et al.* for the amorphous quartz sample.¹² Feature A in both spectra of UV- and TH-SiO₂ split into poorly resolved features at ~ 106.3 and 106.7 eV with a splitting of 0.4 eV, which were well resolved in the spectrum of α -SiO₂ obtained by Wu *et al.*¹¹ The double-split feature A appears as a spin-orbit doublet associated with the transitions of Si $2p_{3/2}$ and $2p_{1/2}$ core states to the antibonding Si $3s$ derived states. Based on SiO₂ cluster models containing 5, 21, and 57 atoms and the multiple scattering theories, Wu *et al.*¹¹ attributed feature B to the tetrahedral symmetry allowed Si $2p$ -to- $3p$ transition. On the other hand, based on the bulk-solid model and the golden-rule scattering theory, which includes electron-hole couplings, the XANES spectrum calculated by Mo and Ching for α -SiO₂ (Ref. 10) agrees much better with the experimental data. Since the scattering theory employed by Mo and Ching obeys dipole transition selection rule, feature B should be assigned to Si $3s$ or $3d$ derived states resulted from hybridization with O $2p$ orbitals. Feature B in the spectra of SiO₂ thin films (~ 108.5 eV) shifts toward lower energies by ~ 0.5 eV relative to that of α -SiO₂ (~ 109 eV).¹⁰ This shift can be caused by the formation of an amorphous component in the UV- and

TH-SiO₂ films in consistency with the XRD measurements presented below. After the background is subtracted from the spectra using a Gaussian baseline, the intensities of features A and B of UV-SiO₂ are found to be reduced relative to those of TH-SiO₂, as shown in the inset of Fig. 1(a). This finding reveals that the degree of hybridization of Si $3sd$ and O $2p$ states in UV-SiO₂ is reduced with respect to that in TH-SiO₂.

Figure 1(b) displays the normalized O K -edge XANES spectra of UV- and TH-SiO₂ films. The general features of these spectra are similar to those of the reference spectra of α -SiO₂.^{10,11} The spectra show an intense and broad white line formed from three contributions, a, b, and c.^{10,11} Wu *et al.*¹¹ attributed feature a at ~ 538 eV to be a resonance that arises from multiple scattering inside two adjacent tetrahedrons with constructive interference and feature b at ~ 540 eV to be associated with octahedral bonding based on cluster models with very small sizes. However, Mo and Ching used the bulk-solid model, which contains only tetrahedral O sites, also obtained feature b, so that the assignment of feature b to octahedral bonding by Wu *et al.*¹¹ may not be the case. Feature b was also observed by Lin *et al.*¹³ in a sample of quartz. Feature c observed in the spectrum of α -SiO₂,^{10,11} which can also be attributed to O $2p$ -Si $3sp$ hybridization, is not well resolved in the spectra of UV- and TH-SiO₂ films, suggesting the formation of larger disordered structures in UV- and TH-SiO₂ films.¹⁴ A higher degree of disorder in UV-SiO₂ can be understood by that the gas-phase Si and O source species stick to the film too fast to be relaxed into a crystalline atomic arrangement during the growth process. The relatively low substrate temperature, typically 380–450 °C, is chosen to optimize the competing processes, i.e., the formation of “metastable” densified SiO₂ and subsequent thermal relaxation into a conventional structure. A Gaussian baseline (represented by a dotted line) was used to subtract the background of the spectra as shown in Fig. 1(b). The inset of Fig. 1(b) indicates that the intensity of the white line feature of UV-SiO₂ is higher than that of TH-SiO₂, suggesting stronger coupling between O $2p$ and Si $3p$ states in UV-SiO₂ than in TH-SiO₂.

Figure 2 presents the VB-PES spectra of UV- and TH-SiO₂ films obtained at excitation energy of 130 eV. The general spectral features of UV- and TH-SiO₂ are similar to those obtained in earlier investigations of SiO₂ films presented elsewhere.^{15–17} In these spectra, $E_B=0$ corresponds to the edge of the valence band and is referred to as the valence-band maximum (VBM). The spectrum of UV-SiO₂ was decomposed into four Gaussian features as shown in the bottom of Fig. 2. The most intense feature in the valence band, feature I, is in the range of 4–10 eV below VBM and centered at ~ 7.5 eV; it is due to the O $2p$ lone pair, i.e., the nonbonding, orbital (marked by blue color shown in the upper inset of Fig. 2), which is perpendicular to the Si–O–Si chain. Feature II lies within the range of 7.5–15 eV; it is centered at ~ 11 eV and is associated with the O $2p$ -Si $3p$ bonding state. Feature III centered at ~ 14.5 eV is associated with the O $2p$ -Si $3s$ states. A combination of features II and III is typically associated with strong Si–O–Si bonding states.¹⁶ Just below VBM there is feature IV in the range of 0–5 eV; the area under this feature is related to the number

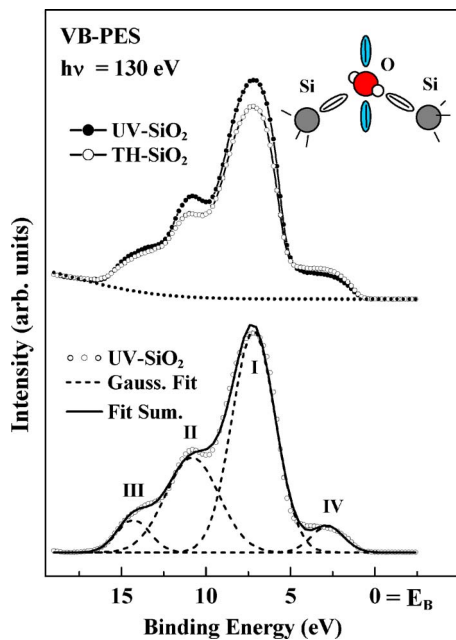


FIG. 2. (Color online) Valence-band photoemission spectra of UV- and TH-SiO₂ films. The valence-band of UV-SiO₂ shown in the bottom is decomposed into four Gaussian peaks, after the Gaussian base subtraction as shown in figure (represented by a dotted line). The upper inset presents the molecular bonds in the SiO₂ tetrahedron.

of Si 3*p* states associated with the Si–Si bonds in the Si substrate and the SiO_x layer at the interface. This feature was also observed by Renault *et al.*¹⁷ Since the intensities of feature IV of both UV- and TH-SiO₂ films are almost equal, the substrate/interface effects are the same in both UV-SiO₂ and TH-SiO₂ films, although the thickness of TH-SiO₂ (50 nm) is ten times larger than that of UV-SiO₂ film (5 nm). According to the density of states of 4:2 coordinated SiO₂ units (Si bonded to four O atoms and O bonded to two Si atoms) as in most SiO₂ polymorphs, the relative intensities of different features of VB-PES in Fig. 2, which are associated with the modifications of various bonding coordinations, especially variations in the intensities of features I and II, are strongly related to O 2*p* nonbonding and O 2*p*–Si 3*p* bonding states.^{16,18} The intensity of feature I in the VB-PES spectrum of UV-SiO₂ is higher than that of the TH-SiO₂ film, which indicates an increase of the number of O 2*p* nonbonding states and a more disordered structure in UV-SiO₂, because disorder gives rise to more dangling bonds (i.e., nonbonding orbitals).¹⁹ The higher intensity of feature II for UV-SiO₂ implies a larger number of O 2*p*–Si 3*p* hybridized states in UV-SiO₂ than in TH-SiO₂. This result is consistent with the larger intensity of the near-edge absorption feature at the O *K*-edge for UV-SiO₂ than for TH-SiO₂, as presented in Fig. 1(b). An enhancement of the O 2*p* and Si 3*p* hybridization in UV-SiO₂ indicates a shortening of the Si–O bond length, which implies an increase of the average density of the UV-SiO₂ film, being 2.32 versus 2.20 g/cm³ of TH-SiO₂. (Note that the O 2*p*–Si 3*s* hybridization, which is reflected in feature III, is less affected by the change of the Si–O bond length because the dominant part of the Si 3*s* orbital lies further into the interior of the Si atom than the 3*p* orbitals.) The polarizability and the dielectric constant depend on the

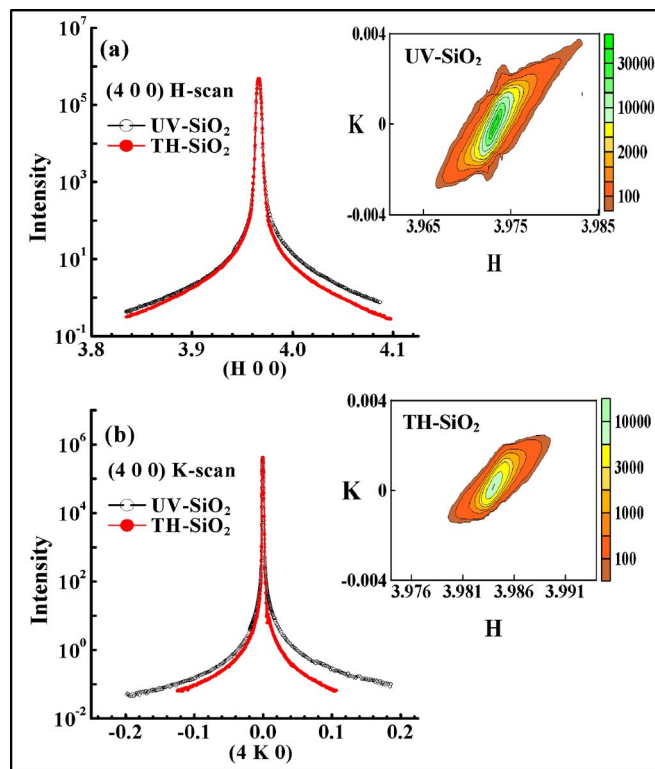


FIG. 3. (Color online) (a) and (b) show linear scans through the Bragg reflection (400) of the Si substrate along the *H* and *K* directions for both UV- and TH-SiO₂ films using high resolution x-ray diffraction, respectively. The intensities are displayed on a log scale. The insets show the contour plots around the (400) of the Si substrate in the *H*-*K* plane.

integration of the product of the density of states and the absolute square of the dipole transition matrix elements between occupied valence-band states and unoccupied conduction-band states. The shortening of the Si–O bond length increases the overlap integrals between Si and O orbitals and consequently the dipole transition matrix elements between these orbitals, while the enhancement of VB-PES features for UV-SiO₂ means an increase of the density of valence-band states. Thus, our results imply an increase of the polarizability and the dielectric constant. Ramos *et al.* suggested that the dielectric properties of SiO₂ polymorphs are related to the position of oxygen and that the dielectric constants increase with the mean Si–O–Si bond angle.²⁰ In contrast, Xu and Ching found that the correlation between the dielectric constant and the bond angle is weak.¹ The present study suggests that the enhancement of the dielectric constant in UV-SiO₂ is due to the shortening of the average Si–O bond length. The shortening of the Si–O bond can be quantitatively evaluated by Fourier analysis of the Si *K*-edge extended x-ray absorption fine structure; measurements are under way.

Both samples were further characterized by x-ray diffraction to verify the structural ordering.²¹ Figures 3(a) and 3(b) present linear scans through the Bragg reflection (400) of the substrate along the *H* and *K* directions on both samples. For comparison, the intensities of UV- and TH-SiO₂ were normalized and the positions were shifted such that the two peaks coincide. The diffraction data clearly show that the reflection is mainly from the Si substrate without signifi-

cant evidence of long-range ordered structure in both SiO₂ films, confirming that UV- and TH-SiO₂ were formed in the amorphous structure. Importantly, Figs. 3(a) and 3(b) show broader shoulders on both sides of the reflection (400) of the Si substrate along the *H* and *K* scans, respectively, indicating that a very short-range-ordered structure was buried in the long-range-ordered Si substrate. This short-range-ordered structure was in both UV- and TH-SiO₂ films. The shoulders of UV-SiO₂ were obviously larger than those of TH-SiO₂. The insets of Fig. 3 display the contour plots around the (400) of the Si substrate in the *H-K* plane, which also shows similarly broader contours for the UV-SiO₂ film. This result further confirms the larger disorder in UV-SiO₂ than in TH-SiO₂. A large degree of structural disorder implies the presence of local strain due to the change of bond lengths or bond angles. Although the energy of bond bending is usually smaller than that of bond stretching, Si and O ions may not have enough relaxation to assume an optimized bond length during low-temperature growth.

IV. CONCLUSION

In conclusion, the intensities of the features in the Si *L*_{3,2}- and O *K*-edge XANES spectra are reduced and enhanced, respectively, for UV-SiO₂ relative to those of TH-SiO₂. The VB-PES measurements show enhancement of the nonbonding O 2*p* states and the O 2*p*-Si 3*p* hybridized states for UV-SiO₂. The former suggests an increase of the structural disorder and the later suggests an enhancement of O 2*p*-Si 3*p* hybridization and a shortening of the average Si-O bond length, forming denser Si-O-Si clusters. Higher density and the enhancement of valence-band states may explain the improvement of the dielectric property of UV-SiO₂.

ACKNOWLEDGMENT

One of the authors (W.F.P.) would like to thank the National Science Council of the Taiwan for financially supporting this research under Contract No. NSC 96-2112-M032-012-MY3.

- ¹Y. N. Xu and W. Y. Ching, Phys. Rev. B **44**, 11048 (1991); M. Z. Huang and W. Y. Ching, *ibid.* **54**, 5299 (1996).
- ²J. Sarnthein, A. Pasquarello, and R. Car, Phys. Rev. Lett. **74**, 4682 (1995); A. Pasquarello and R. Car, *ibid.* **79**, 1766 (1997).
- ³A. Fukano and H. Oyanagi, J. Appl. Phys. **94**, 3345 (2003); A. Fukano and H. Oyanagi, MRS Symposia Proceedings No. 751 (Materials Research Society, Pittsburgh, 2003), p. 61.
- ⁴K. Hirose, H. Kitahara, and T. Hattori, Phys. Rev. B **67**, 195313 (2003).
- ⁵F. Giustino, P. Umari, and A. Pasquarello, Phys. Rev. Lett. **91**, 267601 (2003).
- ⁶H. Momida, T. Hamada, Y. Takagi, T. Yamamoto, T. Uda, and T. Ohno, Phys. Rev. B **73**, 054108 (2006); **75**, 195105 (2007).
- ⁷H. Jin, S. K. Oh, H. J. Kang, and M.-H. Cho, Appl. Phys. Lett. **89**, 122901 (2006).
- ⁸K. Tomida, K. Kita, and A. Toriumi, Appl. Phys. Lett. **89**, 142902 (2006).
- ⁹P. Broqvist and A. Pasquarello, Appl. Phys. Lett. **90**, 082907 (2007).
- ¹⁰S. D. Mo and W. Y. Ching, Appl. Phys. Lett. **78**, 3809 (2001).
- ¹¹Z. Y. Wu, F. Jollet, and F. Seifert, J. Phys.: Condens. Matter **10**, 8083 (1998).
- ¹²G. R. Harp, D. K. Saldin, and B. P. Tonner, J. Phys.: Condens. Matter **5**, 5377 (1993).
- ¹³J. F. Lin, H. Fukui, D. Prendergast, T. Okuchi, Y. Q. Cai, N. Hiraoka, C. S. Yoo, A. Trave, P. Eng, M. Y. Hu, and P. Chow, Phys. Rev. B **75**, 012201 (2007).
- ¹⁴S. Toyoda, J. Okabayashi, H. Kumigashira, M. Oshima, K. Yamashita, M. Niwa, K. Usuda, and G. L. Liu, J. Appl. Phys. **97**, 104507 (2005).
- ¹⁵B. Fischer, R. A. Pollak, T. H. DiStefano, and W. D. Grobman, Phys. Rev. B **15**, 3193 (1977).
- ¹⁶G. Hollinger, S. J. Sferco, and M. Lannoo, Phys. Rev. B **37**, 7149 (1988).
- ¹⁷O. Renault, N. T. Barrett, D. Samour, and S. Quiais-Marthon, Surf. Sci. **566-568**, 526 (2004).
- ¹⁸T. H. Distefano and D. E. Eastman, Phys. Rev. Lett. **27**, 1560 (1971).
- ¹⁹E. Martinez and F. Ynduráin, Phys. Rev. B **24**, 5718 (1981).
- ²⁰L. E. Ramos, J. Furthmüller, and F. Bevhstedt, Phys. Rev. B **69**, 085102 (2004).
- ²¹C. H. Du (unpublished).